Quantum Electronics **37** (8) 784 – 791 (2007)

INTERACTION OF LASER RADIATION WITH MATTER. LASER PLASMA

PACS numbers: 52.57.Fg
DOI: 10.1070/QE2007v037n08ABEH013469

Model of mixing of shells of a thermonuclear laser target upon spherical compression

N.V. Zmitrenko, N.G. Proncheva, V.B. Rozanov, R.A. Yakhin

***Abstract*. Based on many direct numerical simulations of the development of hydrodynamic instabilities upon compression of laser thermonuclear targets, an efficient model is developed for describing the width of the mixing region taking into account the influence of the initial conditions on the mixing process dynamics. Approaches are proposed which are based on the evolution theory of the development of hydrodynamic instabilities [1], which was specially elaborated to describe the compression of targets for inertial thermonuclear fusion.**

Keywords: *inertial confinement fusion, laser target, spherical compression, hydrodynamic instabilities, mixing zones of target shells.*

1. Introduction

The dynamics of the development of a turbulence at the interface of two media with densities ρ_1 and ρ_2, corresponding to light and heavy gases, and the laws of growing the width of the mixing zone appearing here have been studied in many theoretical and experimental papers [1 – 16]. Theoretical investigations were mainly devoted to the analysis of the developed turbulence stage [5 – 14]. The development degree of the turbulence produced by the Richtmayer – Meshkov (RM) or Rayleigh – Taylor (RT) instabilities can be characterised, for example, by the value γt, where $\gamma = (kgA)^{1/2}$ is the characteristic increment of the development of a hydrodynamic instability; $k = 2\pi/\lambda$ is the wave number of a harmonic with the wavelength λ; g is the acceleration produced by an external field; $A = (\rho_2 - \rho_1)(\rho_2 + \rho_1)^{-1}$ is the Atwood number; and t is the evolution time of the initial perturbation.

In the present paper, we propose the method for describing processes corresponding to the condition $\gamma t \leqslant 10$, which follows, as shown below, from spatial and temporal scales that are typical for targets for inertial confinement fusion (ICF). The well-known models describing the turbulent mixing zone [5 – 11] correspond to the values $\gamma t \geqslant 50$ and cannot be directly used to describe the compression of laser targets. At the same time, the problem of the target compression is a specific and quite certain problem. To describe the specific conditions produced upon laser compression of ICF targets, it necessary to characterise briefly this problem.

The advantages of using laser radiation to initiate thermonuclear reactions are the possibilities of its simple focusing and transport to a target and obtaining high power densities required for the efficient target compression. The parameters of high-power Nd laser facilities for irradiating thermonuclear targets operating and being developed in leading laboratories over the world are presented in Table 1.

Table 1. High-power laser facilities for laser thermonuclear fusion (LTF).

LTF facilities	Facility parameters			
	Radiation frequency	Pulse energy	Number of beams	Type of experiment
NIF (USA)	3ω	1.8 MJ	192	Indirect compression
LMJ (France)	3ω	2 MJ	240	Indirect compression
Omega (USA)	$1\omega - 3\omega$	60 kJ	60	Direct compression
Iskra-6 (Russia)	$1\omega - 3\omega$	300 kJ	128	Indirect compression

These facilities are intended and used for experiments on target compression for obtaining a high fusion yield, which depends obviously on the compression conditions and the degree of development of the mixing zone.

Numerous investigations of the interaction of laser radiation with targets showed that it is well absorbed by the evaporating material of the target shell up to power densities $(2 - 4) \times 10^{14}$ W cm^{-2} required for initiating thermonuclear reactions. The absorption coefficient can achieve 40 % – 80 % and decreases with decreasing the radiation wavelength. A high fusion yield can be achieved only if the main part of a fuel contained in the target remains cold during compression. For this purpose, the compression should be adiabatic, i.e. it is necessary to avoid the preliminary heating of the target, which can occur due to laser-induced generation of high-energy electrons, shock waves or hard X-rays. Numerous studies have shown that these undesirable effects can be weakened by distributing the absorbed energy over the target surface, optimising targets, and decreasing the radiation wavelength.

At the same time, the principal problem, whose solution

N.V. Zmitrenko, N.G. Proncheva Institute of Mathematical Modelling, Russian Academy of Sciences, Miusskaya pl. 4a, 125047 Moscow, Russia; e-mail: zmitrenko@imamod.ru;
V.B. Rozanov, R.A. Yakhin P.N. Lebedev Physics Institute, Russian Academy of Sciences, Leninsky prosp. 53, 119991 Moscow, Russia; e-mail: rozanov@sci.lebedev.ru

Received 18 October 2006; revision received 26 January 2007
Kvantovaya Elektronika **37** (8) 784 – 791 (2007)
Translated by M.N. Sapozhnikov

would allow the demonstration of the controllable thermonuclear reaction based on inertial confinement, is the stable compression of a laser target containing a thermonuclear fuel. This can be achieved by providing the uniform heating of the target surface within 1 %–5 %. Such high requirements are determined by the fact that the parameters of target compression required for the demonstration of the controllable thermonuclear reaction appear upon compression along the target radius by a factor of 15–45 [by a factor of $3 \times (10^3 - 10^5)$ in volume] [17].

At present this problem is being studied in the two main directions. One of them involves the symmetric direct irradiation of a shell target of the conventional design by many (a few tens) laser beams. The other direction (indirect compression) is based on the conversion of laser radiation to a beam of thermal X-rays. In both cases, the initiation of a thermonuclear reaction is prevented by the hydrodynamic instability. The development of mixing reduces the fuel temperature and the density of materials being compressed, resulting in a decrease in the neutron yield.

The initial perturbations of ICF targets caused by their compression are determined both by the symmetry and uniformity of the energy source (laser or ion beams, pulsed systems) and the uniformity and manufacturing quality of a target itself. The design of the laser system used for irradiation of targets and the manufacturing technology of targets also play a considerable role. The simulation and theoretical study of the compression of thermonuclear targets are complicated by the necessity of the complex initial spectrum of perturbations, the time-dependent acceleration, etc. However, the consideration of the initial conditions is fundamentally important in the development of mixing models, which would pretend to the correct description of the achievable parameters of a thermonuclear target.

The authors of recent paper [18] presented the data confirming the necessity of taking into account all the above-mentioned mixing conditions in the description of the real compression parameters of targets. On the Omega laser facility (Rochester University, USA), targets of two types were investigated. In the first case, a spherical target had a 15-μm-thick polystyrene shell covered with an aluminium layer and filled with gas (tritium). In the second case, a 1-μm-thick deuterated plastic layer was deposited on the internal surface of polystyrene. The gas pressure inside the target was about 10 atm, and the target compression was performed by laser radiation of a 23-kJ laser pulse. Note that the Omega facility provided the record high irradiation symmetry of the laser target upon direct compression.

The thermonuclear reaction accompanied by the creation of neutrons was initiated in these targets by laser radiation when the target temperature achieved ~ 1 keV. In the first target, neutrons were produced only in the reaction $\mathrm{T} + \mathrm{T} \rightarrow \alpha + 2\mathrm{n} + 11.3$ MeV.

In the second case, upon mixing of tritium with a deuterated plastic shell, the reaction $\mathrm{T} + \mathrm{D} \rightarrow \alpha + \mathrm{n} +$ 17.6 MeV is initiated, resulting in the increase in the neutron yield approximately by two order of magnitude (from 10^{11} up to 10^{13} neutrons). This experiment clearly demonstrates the necessity of taking mixing into account and the development of correct models of the mixing process.

The aim of the present paper is to construct an analytic model based on numerical calculations for describing the development of hydrodynamic instabilities affecting the neutron yield.

We restricted our consideration to the study of a number of 'plane' and 'spherical' problems with certain initial conditions. In the case of the plane problem, two pairs of gases typical for experiments in shock tubes were considered (Xe–Ar or Xe–He at pressures ~ 1 atm, densities $10^{-3} - 10^{-4}$ g cm^{-3} and acceleration 10^7 cm s^{-2}). The shape of the contact surface was described by a sum of harmonics with randomly selected phases, and calculations were performed for a set of 6, 8 or 10 harmonics. The spherical problem had the model nature and contained a small number of harmonics; the calculation parameters corresponded to the laser compression regime (pressure was 10^7 atm, density $1-100$ g cm^{-3}, acceleration $10^{16} - 10^{18}$ cm s^{-2}). Calculations were performed taking into account the substance compressibility and the spherical convergence of the target shells.

Note that considerable differences between calculation parameters for gases in shock waves and for targets compressed by laser radiation do not prevent the construction of the unified model because these gas-dynamic problems take into account the fundamental laws of the gas-dynamic similarity.

By using the calculation base [2] and theory [1], we constructed the model of the development of the mixing zone taking into account the initial perturbation conditions. A part of the results related to analysis of plane problems and the derivation of expressions for the mixing-region width were reported earlier in [2].

It is necessary to explain why we decided to develop a new model of mixing instead of the known models [9, 10].

First, as follows from calculations and theoretical analysis, the acceleration braking the shell of laser targets is virtually always described by the expression $a = 2R/t^2$, where R is the minimal radius of the shell. Then,

$$(\gamma t)^2 = kgAt^2 = \frac{l}{R}\frac{2R}{t^2}At^2 = 2lA,$$

where $l = 2\pi R/\lambda$ is the number of the spherical perturbation mode. It follows from this that $\gamma t < 10$, at least for $l < 50$, and $\gamma t < 20$ for $l < 200$. In our opinion, the influence of harmonics with higher numbers is insignificant because they cease to grow comparatively early already at a small amplitude [1]. However, models [5–8] assume that turbulence is much more developed; in this case, the overestimated width of the mixing zone is obtained, as a rule, so that the results reported in [9, 10] are qualitative, as pointed out in these papers.

Second, the determination of the mixing-zone width is only the first part of the problem. It is necessary to develop then a model taking into account reactions proceeding in a mixed layer depending on the distributions of the fuel concentration, density, and temperature.

Note that the thermonuclear burning occurring under conditions produced due to the development of hydrodynamic instabilities and mixing can be simulated by using direct multidimensional numerical calculations (see, for example, [16]). This method is gradually entering the modern practice of numerical calculations. The problem in this case is how accurately the selected difference scheme mesh will describe the burning and mixing processes in the

presence of the complex initial spectrum of hydrodynamic and thermal perturbations.

2. Numerical calculations in the plane case

The influence of various initial conditions on the development of a turbulence caused by the RT and RM instabilities in the plane geometry was systematically studied earlier by using simulations based on the NUT numerical code [19]. The following plane problem was considered: in the two-dimensional region $\{x_1 \leqslant x \leqslant x_2,\ z_1 \leqslant z_2\}$ of dimensions $x_2 - x_1 =$ 72 mm and $z_2 - z_1 =$ 150 mm, we have $z_1 = -100$ mm, and $z_2 = 50$ mm. The equilibrium distributions of the pressure and density at temperature T_0 are specified at the initial instant of time for two gases in the field of a constant external force (Fig. 1).

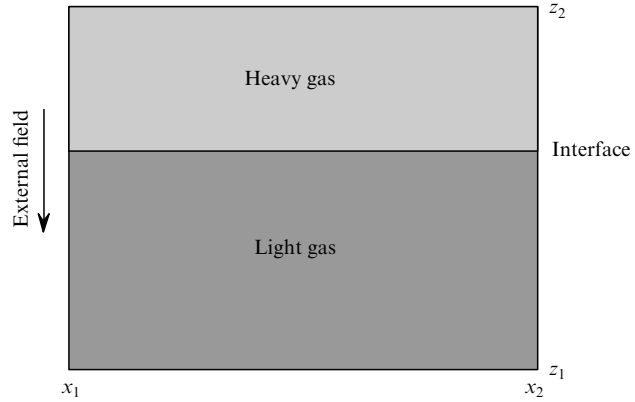

Figure 1. Geometry of the problem.

In the absence of perturbations, the interface of two gases has the coordinate $z = 0$. A heavy gas is located above it in the region $0 \leqslant z \leqslant z_2$, and a light gas is located below in the region $z_1 \leqslant z \leqslant 0$. The acceleration $g = 9.8 \times 10^6$ cm s^{-2} produced by the external force is directed downward. The corresponding distributions of the pressure and density have the form

$$p_i(z) = p_0 \exp\left(-\frac{m_i g z}{\kappa T_0}\right),$$

$$\rho_i = \rho_{0i} \exp\left(-\frac{m_i g z}{\kappa T_0}\right),$$

where $i = 1, 2$ correspond to the light and heavy gases; ρ_{0i} and p_0 are the pressure and density of gases at the interface; m_i is the mass of a gas molecule; $T_0 = 300$ K is the gas temperature taken in accordance with experimental conditions in shock tubes [20]; and k is the Boltzmann constant. For the two selected pairs of gases (Xe–Ar and Xe–He), we have $p_0 = 0.5$ atm, $\rho_{01} = 8.07 \times 10^{-4}$ g cm^{-3} (argon), $\rho_{01} = 8.07 \times 10^{-5}$ g cm^{-3} (helium), and $\rho_{02} = 2.64 \times 10^{-3}$ g cm^{-3} (xenon). These gases are considered in the NUT program as ideal nonviscous gases with the same ratio of specific heat equal to 5/3. Note that under the selected physical conditions, the gas compressibility will affect the process dynamics: the change in pressure with height for the heavy gas achieves 25 %. Perturbations were specified in accordance with the expression

$$z(x) = -\sum_{i=1}^{n} a_{0i} \cos(k_i x + \varphi_i) \tag{1}$$

for the shape of the contact surface. Here, i runs through 6, 8 or 10 values (according the number of generated perturbation modes); $k_i = 2\pi/\lambda_i$ is the wave number of the harmonic with the wavelength λ_i; a_{0i} is the initial amplitude of an individual perturbation; and φ_i is the phase. The wavelengths in (1) were selected from the condition of the absence of harmonics with multiple numbers in the set according to the definition

$$\lambda_i = \frac{x_2 - x_1}{n_i}, \tag{2}$$

where n_i is a simple ith integer ($n_i = 2,\ 3,\ \ldots,\ 29$); and $x_2 - x_1 =$ 72 mm. As a result, the wavelength range was defined as $2.531 \leqslant \lambda_i \leqslant 36$ mm. The initial width L_{0i} of the mixing zone for the ith harmonic was $2a_{0i}$. The amplitudes a_{0i} used in calculations were selected according to one of the main rules (two series of calculations):

(i) $a_{0i} = \alpha_0 \lambda_i / 2\pi$, $\alpha_0 = \text{const}$. The values $\alpha_0/2$: 0.2, 0.5, and 0.8 were used in calculations.

(ii) $a_{0i} = a_0 = \text{const}$ (values $a_0 = 9/\pi$, $L_0 = 2a_0 = 18/\pi$ were used).

Figure 2 presents the result of calculations for a pair of gases He–Xe with six harmonics and the initial amplitude described by the expression $a_{0i} = \alpha_0 \lambda_i / 2\pi$.

The results of this part of studies are presented in paper [2], and they can be briefly formulated as follows:

(i) Based on numerical calculations, the extensive data base is created which describes the development of instability and mixing of two gases in the plane geometry at a constant acceleration for regimes with different instabilities (RT and RM), different Atwood numbers (0.941 and 0.532), different numbers of considered modes and, correspondingly, different maximum numbers of the shortest-wavelength mode ($n_6 = 13$, $n_8 = 19$ or $n_{10} = 29$), and different initial amplitudes a_{0i} and their dependences on the mode number ($a_{0i} = \text{const}/k_i$ and $a_{0i} = \text{const}$);

(ii) the width of the mixing zone on the stage under study depends considerably on the amplitude of initial perturbations and changes nearly linearly in time;

(iii) the width of the mixing zone weakly depends on the contribution of high modes (decreases somewhat when the high modes are included).

3. Model describing the mixing-zone width

Based on numerical calculations, we developed a theoretical model describing the width and velocity of the mixing zone taking into account the influence of initial conditions.

By using correct asymptotics at the initial and later stages of the process, we can make a number of conclusions: at the initial stage of the process in the presence of high modes, the mixing zone extends quadratically in time, which is predicted by the evolution model of the development of instabilities [1]; at the later stage, the growth rate of the mixing zone tends to a constant limiting value, which is determined by the floating velocity of a light gas bubble (sphere). The size of the bubble is determined by the lowest

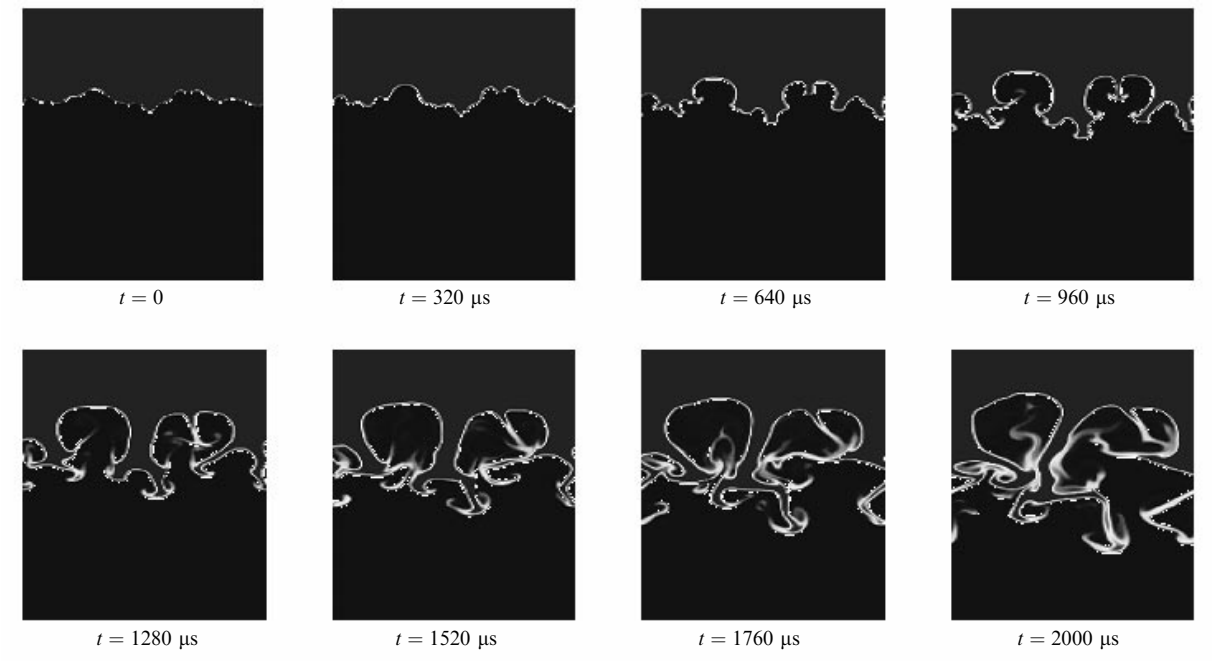

Figure 2. Evolution of the density field (boundary between the heavy and light gases is shown) calculated for the He–Xe pair of gases (plane case, six harmonics).

perturbation harmonic, which has been predominantly developed by this time (according to the Layzer model [21]). The ith harmonic increases the mixing-zone width up to the value

$$L_i(t) = 2a_{0i} + \frac{\lambda_i}{2\alpha_{\text{eff}}}\left\{\left[1 + \frac{(\alpha_{\text{eff}}\gamma_i t)^2}{2\pi}\right]^{1/2} - 1\right\}. \tag{3}$$

Here,

$$\gamma_i^2 = \frac{2\pi}{\lambda_i} gA;\ A = \frac{\rho_2 - \rho_1}{\rho_2 + \rho_1};\ \alpha_{\text{eff}} = \frac{\alpha_0 \alpha^*}{\alpha_0 + \alpha^*};\ \alpha_0 = \frac{2\pi}{\lambda_i} a_{0i}.$$

According to [1], α^* determines the amplitude at which the exponential increase of the instability slows down because mushroom-shaped structures are formed. These structures are distinctly observed in Fig. 2. Usually, for two-dimensional (2D) problems, $\alpha^*_{2D} = 3 - 5$, and for 3D problems, $\alpha^*_{3D} = 10 - 20$.

It is obvious that the mixing-zone width at the initial stage is determined by the amplitude of the linearly developed harmonic. For small t, in accordance with the linear stage of development of instabilities and for the initial development rate equal to zero, we have

$$\frac{\mathrm{d}L_i}{\mathrm{d}t} = a_{0i} k_i g A t = a_{0i}\gamma_i^2 t,\ L_i \sim t^2.$$

For large t, we have

$$\frac{\mathrm{d}L_i}{\mathrm{d}t} = \upsilon\sqrt{g\lambda_i}\,.$$

This quantity in the Layzer model determines the floating velocity of a light bubble $V_{\text{lim}} = \upsilon\sqrt{g\lambda_i}$. Here, $\upsilon(A)$ is the coefficient depending on the problem geometry and the Atwood number A. The coefficient υ in the expression for $\mathrm{d}L_i/\mathrm{d}t$ takes into account the floating velocity and a higher falling velocity of a heavy jet. Typically for 2D problems, $\upsilon = 0.75 - 1$, and for 3D problems, $\upsilon \approx 1 - 1.3$. The mixing-zone width is determined by the contribution from all harmonics; however, it is different and changes with time. At the given moment the long-wavelength perturbations can make the contribution $\sim 2a_i$, and in this case, the short-wavelength perturbations will play a minor role.

We will represent the full width of the mixing zone in the form

$$L(t) = \sum_i L_i(t) w_i(t), \tag{4}$$

where $w_i(t)$ is the weight coefficient determining the contribution of the ith harmonic. At the initial moment, $w_i(0)$ is determined by a random phase of the given perturbation:

$$w_i(0) = \cos(k_i z_1 + \varphi_i) - \cos(k_i z_2 + \varphi_i). \tag{5}$$

Here, z_1 and z_2 are the maximum depths of penetration of the heavy gas into the light gas and of the light gas into the heavy gas, respectively. It follows from (5) that the zone width is determined from the maximum 'high' position of the light gas and the minimum 'low' position of the heavy gas. The value of $w_i(t)$ decreases with time due to the disappearance of the given instability regime and the development of the Kelvin–Helmholtz instability [1]. The behaviour of $w_i(t)$ can be approximately represented by the dependence

$$w_i(t) = w_i(0)\exp[-t(\gamma_{\text{KH}})_i]$$

$$\sim \exp\left[-\frac{1}{4}k_i a_{0i}(\gamma_i t)^2(1-A^2)^{1/2}\right].$$

Here

$$(\gamma_{\mathrm{KH}})_i = k_i v_i \frac{\sqrt{\rho_1\rho_2}}{\rho_1+\rho_2};\ v_i t = \frac{a_{0i}}{2}[\exp(\gamma_i t)+\exp(-\gamma_i t)]$$

$$\approx a_{0i}\left[1+\frac{(\gamma_i t)^2}{2}\right];$$

v_i is the velocity of the shear flow for the ith harmonic caused by the RT instability.

The values of $(\gamma_{\mathrm{KH}})_i$ and γ_i depend on the wave number $k_i = 2\pi/\lambda_i$ and, hence, on the harmonic number. One can see that the contribution to the zone width of the ith harmonic decreases faster with increasing the harmonic number. If the spectrum of initial perturbations is $k_i a_{0i} = \mathrm{const}$, then $w_i(t) \sim \exp(c_1 p_i)$; if the initial perturbations are described by the expression $a_{0i} = \mathrm{const}$, then $w_i(t) \sim \exp(-c_2 p_i^2)$, where c_1 and c_2 are some constants. At later stages, the contribution from high harmonics is not zero and should be taken into account. We can assume that the contribution of the harmonic after its destruction to the zone width will be of the order of the wavelength. Based on the results of calculations and using the fitting method, we proposed the expression

$$w_i(t) = w_i(0)\left\{\frac{2}{p_i}+2\left(1-\frac{2}{p_i}\right)\right.$$

$$\left.\times\left[1+\exp\left(\frac{\lambda_{i_{\max}}^2}{\lambda_i^2}w_i^2(0)\gamma_i^2 t^2\right)\right]^{-1}\right\} \qquad (6)$$

for the weight coefficient of the ith harmonic. The high-frequency modes make contributions to the zone width at the mixing stage. This contribution is of the orders of $(3-5)\lambda_i/2\pi$ and $(10-20)\lambda_i/2\pi$ for the 2D and 3D geometries, respectively [1]. The more important conclusion is that the zone width is mainly determined by the long-wavelength perturbations developed by the given moment. Because the value of $\gamma_i t$ for these perturbations is smaller, their evolution can be simply found by using direct numerical calculations or estimated by using analytic models developed, for example, in [1]. Figures 3 and 4 present the time dependences of the mixing-zone width (the theory described above is compared with numerical calculations [2]). One can see that expressions (3)–(6) well describe the mixing-zone width in plane problems of the RT instability.

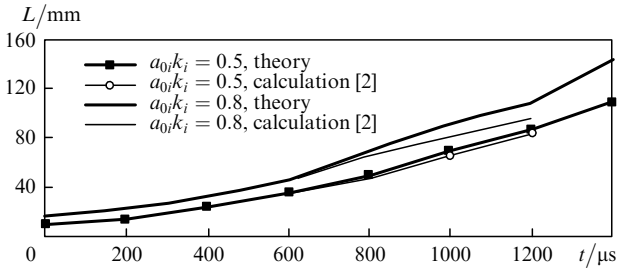

Figure 3. Time dependences of the mixing-zone width for the He–Xe pair of gases for $a_{0i}k_i = 0.5$ and 0.8. Calculations were performed for six harmonics.

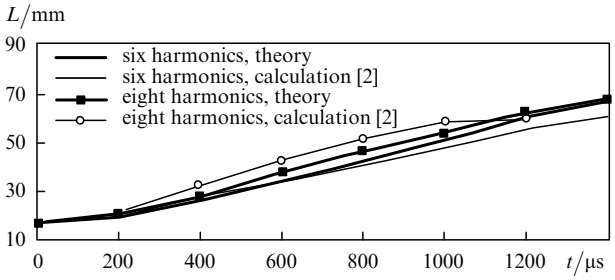

Figure 4. Time dependences of the mixing-zone width for the Ar–Xe pair of gases for $a_{0i} = a_0 = 9/\pi$. Calculations were performed for six and eight harmonics.

Let us characterise briefly the models proposed earlier for the description of the mixing-zone width. It seems that the mixing of two gases with different densities in the gravitational field was first theoretically analysed in paper [3]. The mixing-zone width calculated in this paper (the formulation of the problem was similar to that in our paper) is described by the expression

$$L(t) = \alpha \ln\left(\frac{\rho_1}{\rho_2}\right)\left(\int_0^t \sqrt{g}\,\mathrm{d}t\right)^2, \qquad (7)$$

where α is a constant depending on the type of substances being mixed and the degree of their mutual penetration. In the limit of a small density difference and the constant acceleration g, expression (7) takes the form

$$L(t) = \alpha A g t^2. \qquad (8)$$

The form of expression (8) is determined by the so-called self-similar stage of the development of turbulent mixing [6, 12]. The approach developed in [3] was used later in many papers.

At present, the most popular expression for the mixing-zone width has the form [7]

$$L(t) = L_{\mathrm{b}} + L_{\mathrm{s}} = (\alpha_{\mathrm{b}} + \alpha_{\mathrm{s}})Agt^2, \qquad (9)$$

where the contributions of the penetration of a light substance to a heavy substance (L_{b}) and of a heavy substance to a light substance (L_{s}) are separated.

Note that a new recent tendency appeared in the study of the turbulence caused by the development of the RT and RM instabilities. It is related to new experimental results and calculations (see, for example, [12–14]), which show that either the developed (self-similar) stage appears much later than was expected or the coefficient α changes with time. Such a type of mixing is attributed to the spectrum of initial perturbations, while the change in α is explained by the change in the spectrum during the development of the turbulence. Note that the evolution model [1] takes consistently into account from the very beginning both the initial zone width and the spectrum of perturbations and the evolution of the spectrum during the development of instabilities caused by the saturation of short-wavelength perturbations. Therefore, it is reasonable to use this approach to describe mixing in laser targets.

4. Numerical calculations in the spherical case

The next stage of the study of mixing processes in the ICF problem is numerical calculations of the compression of spherical targets, which are closest to real laser targets, and the attempt to describe them by using the theoretical model proposed above.

A spherical target assumes the existence of a number of new factors which considerably complicate the simulation of the development of the mixing zone. These factors are the finite compression time, the complicated initial perturbation spectrum containing the low- and high-frequency harmonics, which is not always exactly known, the complicated structure of a target itself, a strong nonlinearity of the development dynamics at the later (collapse) stage, etc.

By using the NUT program, we performed a number of calculations with the initial conditions of the same type. Figure 5 presents the cross section of a target consisting of several concentric spherical shells having different functions: the external heavy CH ablator layer (not shown), the next DT fuel layer in the form of ice of density 0.2 g cm^{-3}, and the internal DT gas layer [22].

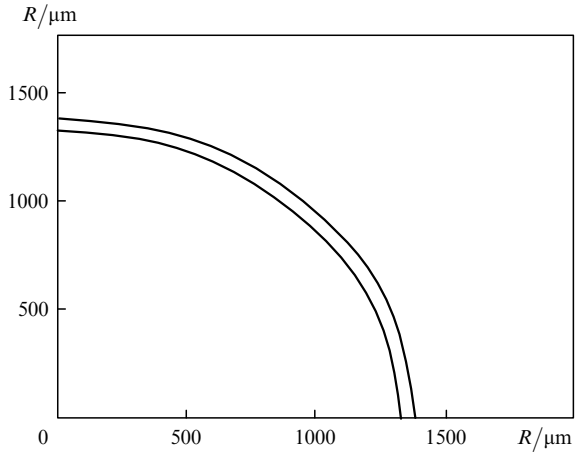

Figure 5. Cross section of the initial spherical target (shown is the position of the DT ice shell).

We considered the compression process for the three last nanoseconds (target at the collapse stage). The density and radius of different layers were: $\rho_{CH} = 12$ g cm^{-3} and $R_{CH} =$ 926 μm for the ablator, $\rho_{DT} = 0.5$ g cm^{-3} and $R_{DT} =$ 916 μm for the DT ice layer, and $\rho_{in} = 3.5\times\ 10^{-5}$ g cm^{-3} and $R_{in} =$ 768 μm for the internal DT gas layer. The instability was specified at the DT ice – internal gas interface (Fig. 6). At the instant $t = 0$, the CH and DT layers began to move toward the centre at the velocity $V_0 = 300$ km s^{-1}, by compressing the target.

Figure 7 presents the results of calculations performed for the 6th and 15th harmonics with the initial amplitudes 4.5 and 18 μm, and for the 48th harmonic with the amplitude 3 μm.

The shape of the contact surface was defined by the expression

$$R = R_{in} + \sum_i a_{0i} \cos(n_i \theta), \tag{10}$$

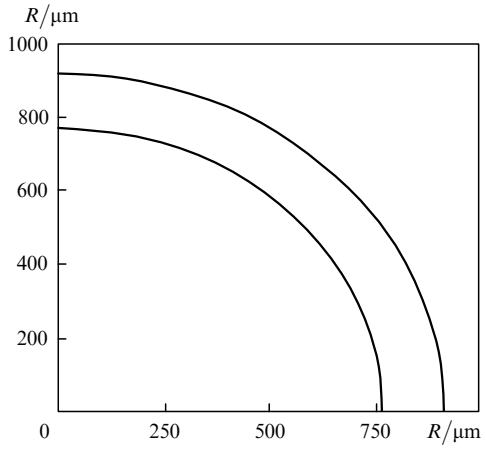

Figure 6. Cross section of a spherical target at the beginning of calculations (for comparison with the initial cross section in Fig. 5). The boundaries and gas densities inside the target and DT layer changed.

where θ is the angle determining the position of a given point on the interface. The target is compressed for 3 ns.

Figure 8 presents the time dependences of the integrated parameters of the compression process obtained in calculations.

Figure 9 compares the mixing-zone width obtained in calculations and by using expressions (3) – (6). The theory based on calculations in the plane case neglects a number of factors related to the spherical shape of targets such as gas compressibility and the target convergence. Their influence was discussed, for example, in paper [15] and later in [23].

The increment of development of the hydrodynamic instability is described by the expression [23]

$$\gamma = 0.5(\gamma_\rho + \gamma_R) + \left[\gamma_0^2 + \frac{1}{4}(\gamma_\rho + \gamma_R)^2\right]^{1/2}, \tag{11}$$

where

$$\gamma_0^2 = \frac{l(l+1)}{R} \frac{(\rho_2 - \rho_1)g}{l\rho_2 + (l+1)\rho_1};\ \gamma_\rho = \frac{\mathrm{d}\rho}{\rho \mathrm{d}t};\ \gamma_R = \frac{\mathrm{d}R}{R\mathrm{d}t};$$

l is the number of harmonics involved in calculations. The theoretical consideration takes into account only γ_0.

In the case $\mathrm{d}\rho/\mathrm{d}t = 0$, i.e. when compression occurs without an increase in density, the spatial amplitude is $a_i \sim R^{-2}$; if $\mathrm{d}(\rho R^3)/\mathrm{d}t = 0$, i.e. when the mass of a substance is preserved, $a_i \sim R$ (the mixing zone narrows down somewhat).

By analysing the calculation results presented in Fig. 7, we can conclude that the compression (γ_ρ) and convergence (γ_R) coefficients are approximately an order of magnitude lower than the classical increment of the instability growth (for example, for calculations with the 6th and 15th harmonics with amplitudes 18 μm, we have $\gamma_0 \approx 10^{10}$ s^{-1}, and $\gamma_\rho \approx 10^9$ s^{-1}, $\gamma_R \approx -10^9$ s^{-1}). This allows us not to include these coefficients in the first approximation in expression (3) for the mixing-zone width, the more so as these compression and convergence effects have opposite signs and partially compensate each other.

Expressions (3) – (6) determining the width of the mixing zone can be easily introduced into one-dimensional codes for calculating the compression and thermonuclear burning of targets.

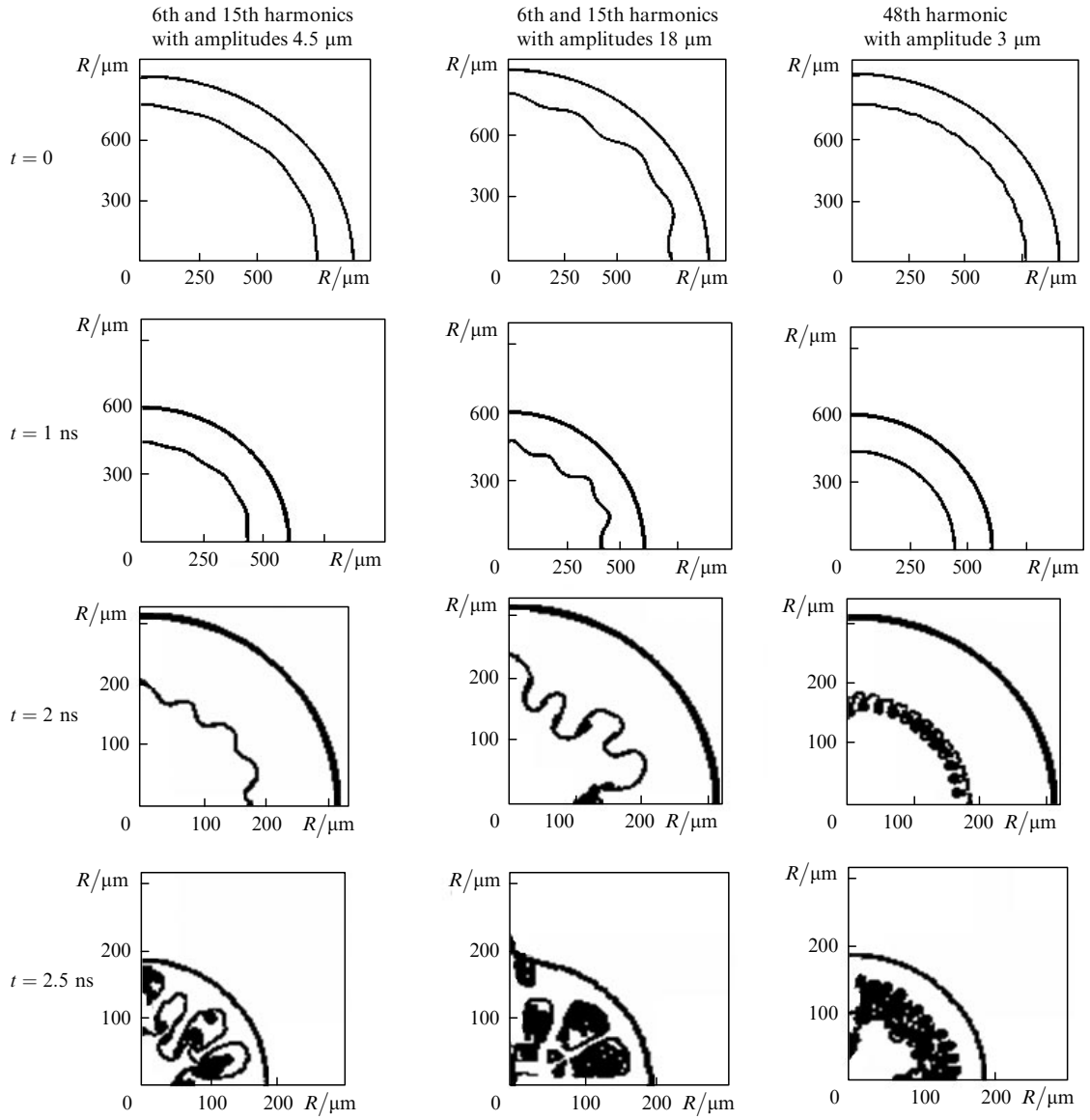

Figure 7. Results of numerical calculations. Shown is the position of the DT ice shell. The scale of figures corresponding to times 2 and 2.5 ns along the x and y axes is enlarged approximately by a factor of three.

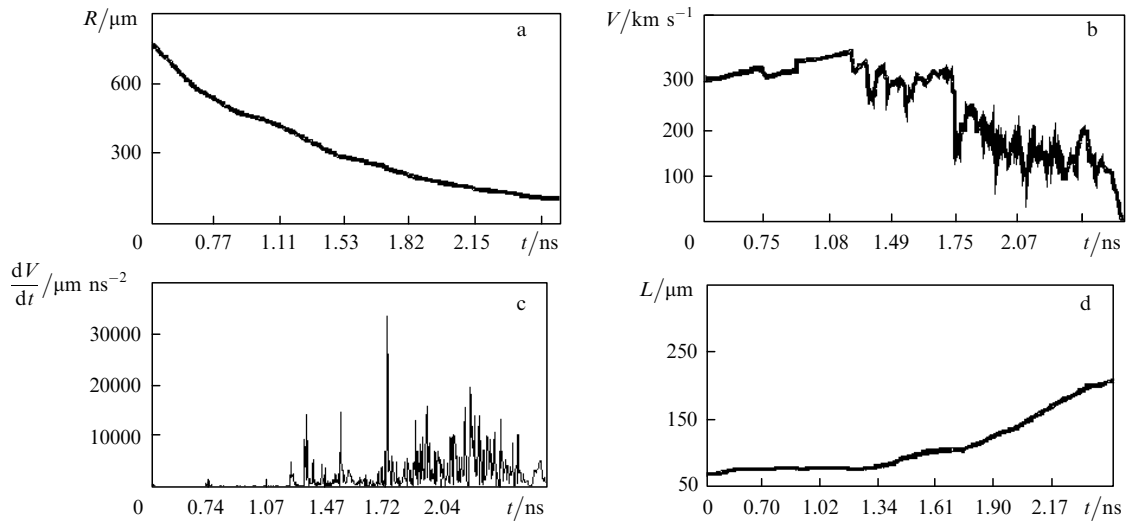

Figure 8. Time dependences of the radius (a), compression rate (b), acceleration (c) of the DT layer and the mixing-zone width (d) (the case of the 6th and 15th harmonics with amplitudes 18 μm).

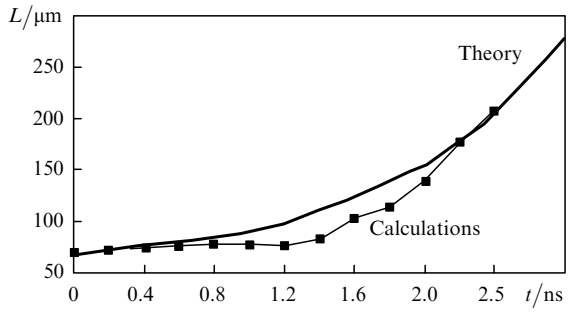

Figure 9. Time dependences of the mixing-zone width for the target presented in Fig. 6. Calculations were performed for the 6th and 15th harmonics with amplitudes 18 μm.

The calculations that we performed contain detailed information on the state of interacting gases, the size of the mixing region, etc. Therefore, we can hope to determine the influence of mixing on the efficiency of thermonuclear reactions more accurately in the future.

5. Conclusions

We have calculated the development of instabilities of the turbulent RT and RM mixing for different initial conditions for the composition of initial perturbation modes, amplitudes, gases involved in mixing, perturbation phases and geometries. Some calculations corresponded to the development of instabilities in shock tubes, while others – to the laser compression regime.

The results of numerical calculations, their processing and the dependences obtained have given the answer to the important question about the dependence of the mixing parameters on the initial conditions upon compression of thermonuclear targets. These calculations have revealed a weak dependence of the mixing-zone width on the contribution of high-frequency modes (this width decreases somewhat with increasing the number of high-frequency modes taken into account).

Based on the study of the development of instabilities in plane and spherical calculations and by using the evolution model of the development of instabilities, we have derived analytic expressions (3)–(6) describing the development of the mixing zone taking into account the initial conditions including the spectrum, perturbation amplitudes, etc.

A comparison of the results of calculations with the predictions of the proposed theory have shown that analytic expressions (3)–(6) are in good agreement with calculations.

An important advantage of the expressions obtained is the possibility of their using for the description of mixing processes in a broad range of physical parameters in calculations simulating fundamentally different regimes.

Acknowledgements. This work was supported by the Russian Foundation for Basic Research (Grant Nos 05-01-00631 and 06-02-91226-yaf).

References

1. Zmitrenko N.V., Proncheva N.G., Rozanov V.B. Preprint FIAN, No. 6 (Moscow, 1997).
2. Rozanov V., Stepanov R., Nuzny A., Yakhin R., Anuchin M., Proncheva N., Zmitrenko N., Yanilkin Yu., Tishkin V. Preprint FIAN, No. 28 (Moscow, 2004).
3. Belen'kii S.Z., Fradkin E.S. *Trudy FIAN*, **29**, 207 (1965).
4. Rozanov V.B., Zmitrenko N.V., Proncheva N.G., Yakhin R.A. Prepring FIAN, No. 28 (Moscow, 2005).
5. Gauthier S., Bonnet M. *Phys. Fluids A*, **2** (9), 1685 (1990).
6. Neuvazhaev V.E. *Matem. Model.*, **3**, 10 (1991).
7. Youngs D.L. *Phys. D*, **12**, 32 (1984).
8. Nikiforov V.V. *VANT, Ser. Teor. Prikl. Fiz.*, (1), 3 (1985).
9. Andronov V.A., Bakhrakh S.M., Mokhov V.N., Nikiforov V.V., Pevnitskii A.V. *Pis'ma Zh. Eksp. Teor. Fiz.*, **29**, 62 (1979).
10. Lykov V.A., Murashkina V.A., Neuvazhaev V.E., Shibarshov L.I., Yakovlev V.G. *Pis'ma Zh. Eksp. Teor. Fiz.*, **30**, 339 (1979).
11. Andronov V.A., Bakhrakh S.M., Mokhov V.N., Nikifotrov V.V., Pevnitskii A.V., Tolshmyakov A.I. *Dokl. Akad. Nauk SSSR*, **264**, 76 (1982).
12. Yanilkin Yu.V., Statsenko V.P., Rebrov S.V., Sin'kova O.G., Stadnik A.L. *VANT, Ser. Matem. Model. Fiz. Prots.*, (2), 3 (2002).
13. Garina S.M., Zmitrenko N.V., Proncheva N.G., Tishkin V.F. *VANT, Ser. Matem. Model. Fiz. Prots.*, (2), 10 (2002).
14. Cabot W., Cook A.W., Miller P.L. *J. Fluid Mech.*, **511**, 333 (2004).
15. Clark D.S., Tabak M. Preprint LLNL (2005).
16. Galmishe D., Cherfils C. *Proc. SPIE Int. Soc. Opt. Eng.*, **5228**, 28 (2003).
17. Rozanov V.B. *Usp. Fiz. Nauk*, **174**, 371 (2004).
18. Wilson D.C., Sangster T.C., Ebey P.S., et al. *Proc. 10 IWPCTM* (Paris, 2006) p. 11.
19. Tishkin V.F., Nikishin V.V., Popov I.V., Favorskii A.P. *Matem. Model.*, **7**, 15 (1995).
20. Aleshin A.N., Lazareva E.V., Chebotareva E.I., Sergeev S.V., Zaytsev S.G. *Proc. VI Intern. Phys. Compressible Turbulent Mixing* (Marseille, 1997) p. 1.
21. Layzer D. *Astrophys. J.*, **122** (1), 1 (1955).
22. Rozanov V., Doskoch I., Guskov S., Stepanov R., Zmitrenko N. *J. Phys. IV France*, **133**, 213 (2006).
23. *LLE 2003 Annual Report* (University of Rochester, 2004) p. 81.